LEVEL II

science applications, inc.

DTIC
S ELECTE D
SEP 3 0 1980
E
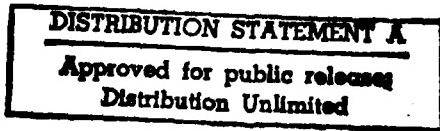
80 8 27 022

(14) SAI202-80-460-LJ

(11) Mar 80   (12) 46

(6)

MIZPAC 80A: USCGC POLAR STAR (WAGB-10)
ARCTIC TEST OPERATIONS,
BERING SEA

CRUISE REPORT AND PRELIMINARY
OCEANOGRAPHIC RESULTS

(10)   J. L. Newton
       B. G. Andersen

Science Applications, Inc.
La Jolla, California

(15) N00014-79-C-0689

Prepared for:

Office of Naval Research
Arctic Programs Code 461

388 862

FOREWORD

This report is intended to provide the Office of Naval Research (Code 461) with a description of the March 1980 Bering Sea Cruise which was conducted as a part of the 1980 Arctic West Operation of the USCGC POLAR STAR (WAGB 10). Some preliminary oceanographic reslts are presented as they relate to the cruise objectives. These results are based on preliminary shipboard data and are by no means in a final form. However, it is anticipated that some of the ideas discussed here will be pursued, in conjunction with the Naval Postgraduate School, as the final data becomes available. Final station plots of temperature and salinity versus depth will be forwarded as a Naval Postgraduate School Technical Report.

Accession For		
NTIS GRA&I	☒	
DDC TAB		
Unannounced		
Justification *Per*		
Letter on File		
By		
Distribution/		
Availability Codes		
Dist.	Avail and/or special	
A		

CONTENTS

LIST OF FIGURES

LIST OF TABLES

1. BACKGROUND

During the March 1980 Bering Sea Cruise of the USCGC POLAR STAR, physical oceanographic and underwater sound studies were conducted as a part of a continuing research program in support of the Navy's Submarine Arctic Warfare Program. The cruise was under the overall direction of the Arctic Submarine Laboratory, a part of the Naval Ocean Systems Center, San Diego, CA, with the participation of scientists from the Naval Postgraduate School, Monterey, CA, the Applied Physics Laboratory, University of Washington, Seattle, WA, and Science Applications, Inc., La Jolla, CA.

Experience has shown that the northern Bering and Chukchi Seas present the most difficult underice operational challenge a submarine crew will face. Comprehensive environmental data are particularly important to safe operation in this shallow water - underice regime. Prior research has concentrated on the dynamics of the ice margin during the summer, emphasizing the interaction of warm waters with the colder water mass under the ice. This interaction can lead to complex sound velocity structures which in turn have adverse effects on ice avoidance sonars and acoustic torpedoes. To supplement these prior summer studies, this cruise was conducted in March, a time of maximum ice cover extent in the Bering Sea.

A major factor influencing wintertime hydrographic structure over majority of the Bering Sea continental shelf is the freezing process with its attendant brine rejection and the convective overturn of the water column under the forming sea ice. As a result the water column within the ice pack is usually vertically homogeneous in both temperature and salinity. Notable exceptions to vertical homogenity occur near the ice margin, in regions influenced by local freshwater addition (meltwater or river discharge), and perhaps in situations where adjacent waters of different salinities may merge laterally to form a layered structure.

The ice margin is a highly dynamic region of particular interest. At the surface, the ice margin marks the transition between the ice-free oceanic waters to the southwest and the nearly continuous March ice pack over the Bering Sea Shelf. The ice edge is often coincident with the subsurface

1

transition between the warmer (and more saline) waters of the Bering Sea and the colder (fresher) waters which occupy the middle and outer shelf regions. The thermodynamic processes within the ice margin, particularly the question of whether ice is melting or freezing there, are important to understanding the overall behavior of the Bering Sea ice pack.

2. CRUISE DESCRIPTION

2.1 SPECIFIC OCEANOGRAPHIC OBJECTIVES

The specific oceanographic objectives for this cruise which in turn support the overall research goals of the Navy Submarine Arctic Warfare Program included:

- Development of descriptive data on the general ocean-ographic conditions of the Bering Sea during the wintertime.

- Definition of any observed phenomena associated with the ice edge, such as temperature-salinity structure, and in particular those features which could impact sound transmission.

- Characterization of the brine convection process with respect to spatial variability, the effect of water depth, the influence of local fresh water additions and regions of more significant ice formation.

- Definition of the spatial influence of low salinity surface water resulting from river discharge.

- Examination of the hydrographic structure of the ice edge to help substantiate recent concepts that the ice edge is a region where significant melting occurs of ice formed in the northern Bering Sea and carried south by winds.

2.2 SCIENTIFIC PARTY

The Chief Scientist and five personnel involved with the physical oceanographic studies boarded the POLAR STAR in Sitka, Alaska on 24 February, 1980. They included:

Dr. M. Allan Beal, Arctic Submarine Laboratory, Chief Scientist
Dr. R. G. Paquette, Naval Postgraduate School
Dr. R. H. Bourke, Naval Postgraduate School
Dr. J. L. Newton, Science Applications, Inc.
Mr. B. G. Andersen, Science Applications, Inc.
Mr. K. O. McCoy, Naval Postgraduate School

The scientists conducting the high frequency underice sound propagation studies embarked at Nome, Alaska on 13 March 1980. They were:

Dr. R. E. Francois, Applied Physics Lab, University of Washington
Mr. G. R. Garrison, Applied Physics Lab, University of Washington
Mr. E. W. Early, Applied Physics Lab, University of Washington

The scientific party was disembarked at Adak, Alaska on 4 April, 1980.

2.3   CRUISE TRACK

The cruise track is represented in Figure 1 as a plot of 0000Z and 1200Z ships positions during the period 29 February through 2 April 1980. After a brief stop in Dutch Harbor, Alaska to investigate future potential fueling sites the ship began its northward transit on 29 February. The ice margin was encountered early on 1 March at about 57°-00' N, 167°-30' W. A line of oceanographic stations were occupied across the ice edge on 1-2 March. The ship continued north, with slow progress especially on 7-10 March, taking oceanographic stations until its arrival in Nome on 13 March. After a brief stop in Nome to embark the scientists for the acoustic experiment, the ship proceeded west along a line north of St. Lawrence Island. Heavy, ridged ice north of St. Lawrence coupled with some engineering problems resulted in very slow progress (about 5 days to cover 100 n.mi.) along this leg of the track.

After rounding the western end of St. Lawrence, the ship proceeded to approximately 62° N, 171°W for the acoustic experiments. During 24-28 March, an ice camp was established in the vicinity of the ship. Personnel from the Applied Physics Laboratory manned the camp daily and conducted a series of high frequency sound propagation tests. During this time periodic oceanographic casts were taken from the ship. On 28 March the ship departed the area of the ice camp and proceeded southwest in the general direction of Adak passing west of St. Matthews Island. The ship exited the ice on 2 April at about 59°-30' N, 171°-00 W. A line of oceanographic stations were occupied across the ice edge.
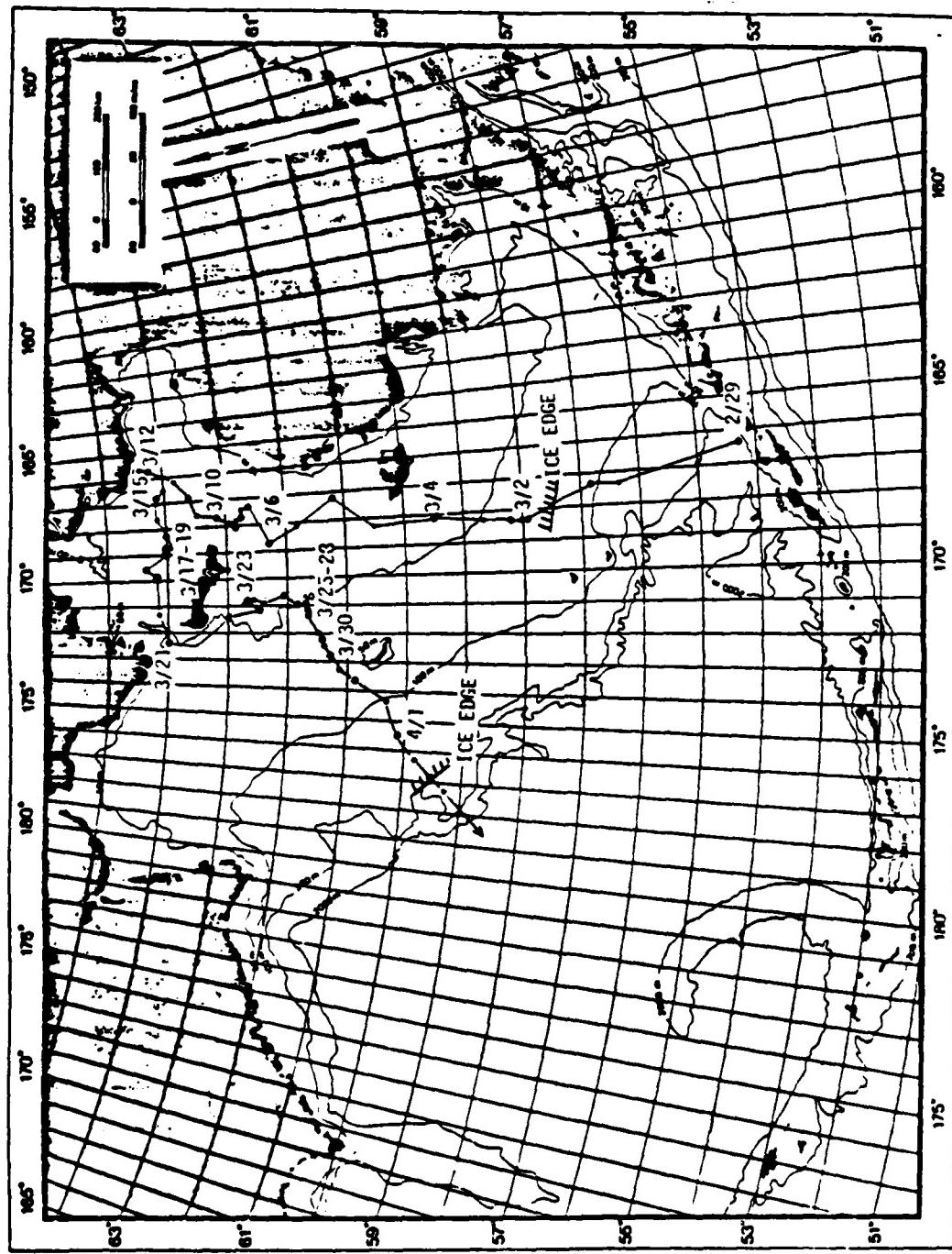
Figure 1. Cruise track of USCGC POLAR STAR for period 29 February - 2 April 1980. The 0000Z (large dot) and 1200Z (small dot) ship positions are plotted daily.

3. INSTRUMENTS AND METHODS

3.1 GENERAL

Two Conductivity-Temperature-Depth (CTD) instrument systems were utilized during the cruise. The primary shipboard instrument was a Neil Brown Instrument MKIII CTD System belonging to the Naval Postgraduate School. This system was deployed using the ship's power winch and single core armored cable. The second system was a Lightweight Profiler developed at the Applied Physics Laboratory, University of Washington. The Lightweight Profiler was usually deployed from a helicopter as it hovered over an opening in the ice or occasionally through a hole drilled in the ice. Some casts were taken from the ship for testing and instrument intercomparisons.

3.2 NEIL BROWN MK III CTD

The Neil Brown CTD was interfaced to a Hewlett-Packard 9835B desktop calculator and a 9872A plotter. The system was programmed to collect 1, 2 or 4 blocks of data with each block consisting of 84 seconds of data (at a lowering rate of 60m/min, this usually covered a depth interval of about 70m). A sample set of conductivity, temperature, oxygen and depth readings were recorded about 14 times per second within each data block. Upon completion of the cast the data were plotted and recorded on tape cartridges. A Nansen bottle with two protected reversing thermometers was placed about 6m above the CTD and tripped at the bottom of the cast to obtain independent checks on temperatures and water samples for shipboard salinity analysis. The comparisons of these calibration samples and the CTD temperatures and salinities were generally quite good with differences falling within the measurement accuracies of the respective methods. Thus, no corrections were applied to the CTD temperature and salinity data utilized here.

3.3 APL LIGHTWEIGHT PROFILER

The Lightweight Profiler is a portable, self-contained, battery-operated system which can be deployed from the ship, from the ice through a drilled hole or from a helicopter hovering over an open water area. Data is recorded internally at a rate of about 3 conductivity-temperature-depth sample

6

sets per second on a tape cassette. Preliminary analysis, salinity computation and plotting is accomplished onboard ship with a Hewlett-Packard 9100 series desktop calculator/plotter system. Comparisons between the Lightweight Profiler and the Neil Brown CTD were made at 8 stations by taking sequential casts at closely spaced time intervals, usually less than 10 minutes. A small temperature and salinity offset with depth was noticed in the Lightweight Profiler data which was traced to a grounding problem, probably in the electrical cable. After correcting the problem and recalibrating the previous casts the comparisons in Table I were obtained using the near surface and near bottom readings at 8 stations (16 comparisons). Of the comparisons, 83% of the differences fell in the range $\pm0.02^{\circ}$C and ±0.02% with a mean temperature difference of 0.005°C and a mean salinity difference of -0.014%.

Table I. Temperature and Salinity Comparisons, 16 Sets

TEMPERATURE (NBIS CTD-LP)		SALINITY (NBIS CTD-LP)	
MEAN	RANGE	MEAN	RANGE
$+0.005^{\circ}$ C	-0.02°C to $+0.03^{\circ}$ C	-0.014%	-0.05% to +0.02%

4. PRELIMINARY RESULTS

4.1 STATION DISTRIBUTION

A total of 83 CTD stations were occupied during this cruise. The positions, dates, times, instrument used and other data are tabulated in Appendix A. The positions are plotted in Figure 2 with the circles indicating shipboard stations and the Δ's denoting casts made from the hovering helicopter with the Lightweight Profiler. For simplicity, the lines of stations made from the helicopter are labeled A through E as follows:

Line A: An east-to-west line from the 10m curve seaward at Latitude about 62°-15'N, consisting of stations 26-29.

Line B: A northeastward tending line from about the 10m contour seaward toward St. Lawrence Island. Stations 30, 31 and 33.

Line C: A continuation of Line B to St. Lawrence Island. Stations 37-39.

Line D: A northeastward oriented line from the 10m contour near the Yukon consisting of stations 43-46.

Line E: An east-west line of three stations (48-50) in Norton Sound.

As indicated on Figure 2 the ice edge was encountered between stations 9 and 10 on the northward transit while station 79 marked the ice edge on the outbound leg.

Ship positions were typically fixed using Loran C although some NAVSAT fixes were obtained on an irregular basis. Helicopter station positions were determined by taking a radar range and bearing from the ship on a high altitude helicopter as it overflew the hovering unit taking the station. On a few occasions helicopter station positions were determined by a Loran C unit onboard the helicopter. Overall, station position accuracy is probably within 1.5 n.m. ($\sim$2km).

4.2 WEATHER AND ICE CONDITIONS

Figure 3 summarizes the weather and ice conditions encountered during the cruise. For convenience, the data are plotted versus time (date)
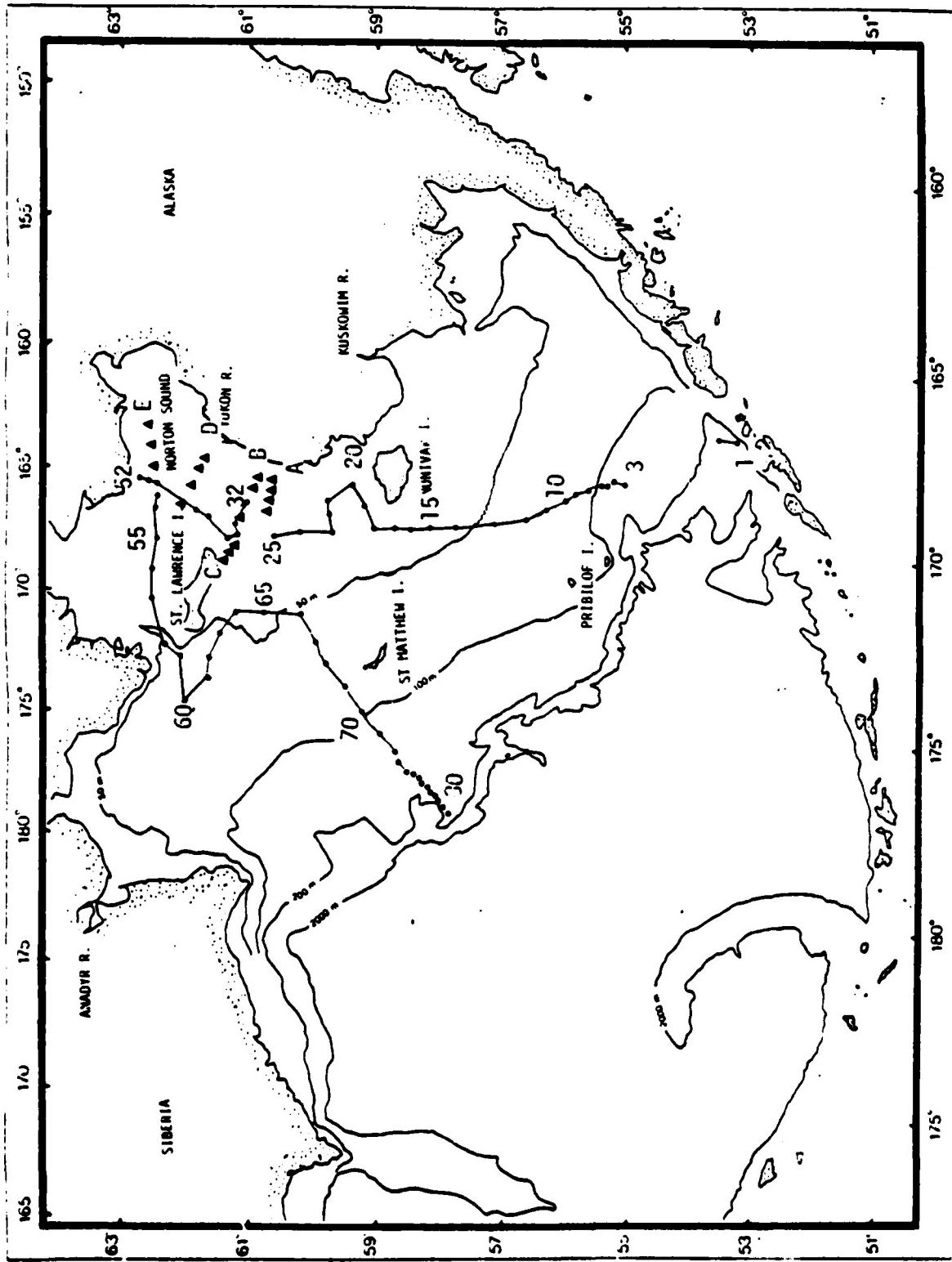
Figure 2. Location of CTD stations. The circles locate shipboard stations and the triangles indicate CTD casts taken from the hovering helicopter. The locations and specific instrumentation are indicated in Appendix A.

9
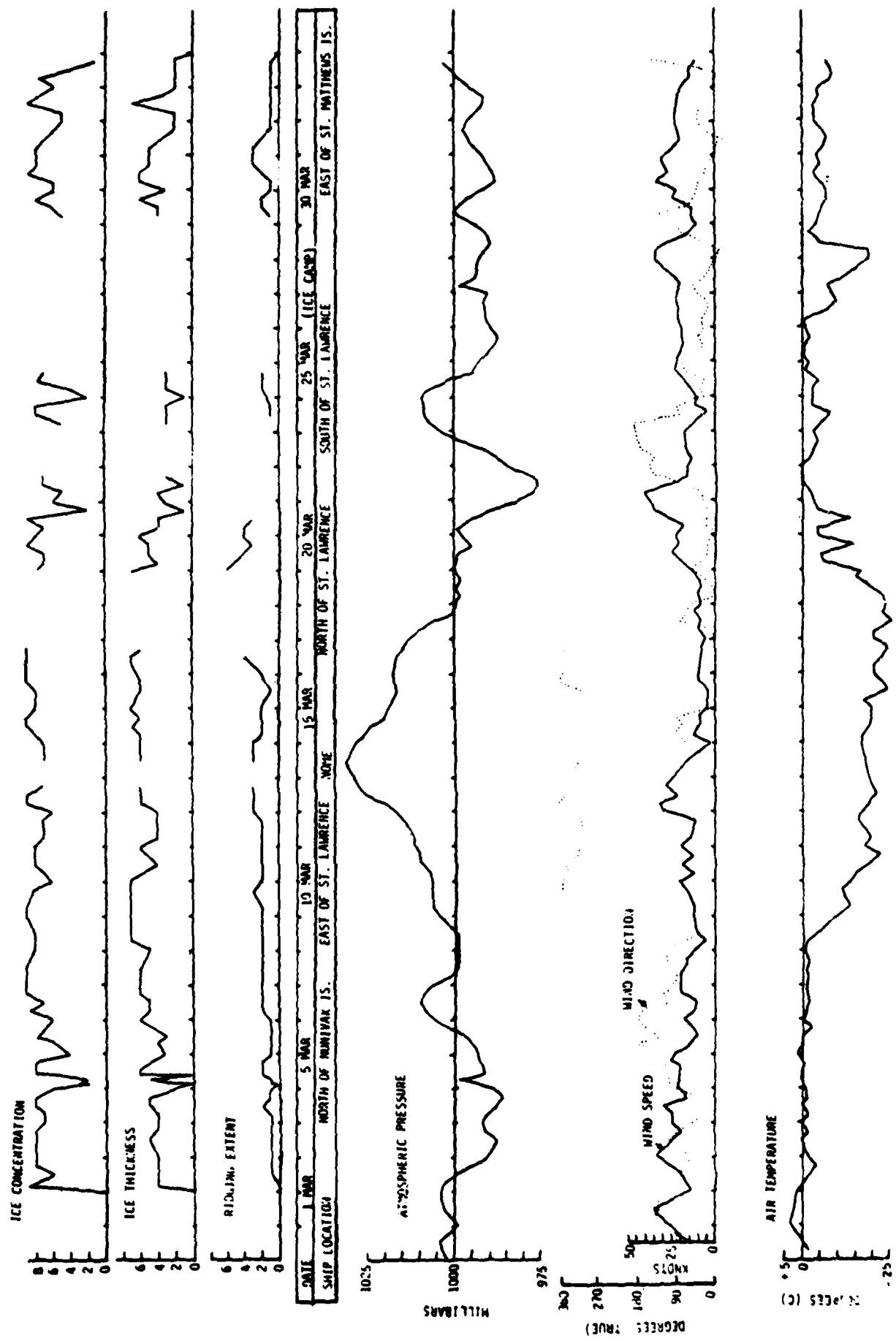
Figure 3. Weather and ice conditions encountered during the cruise. Upper three graphs are ice concentration, thickness and ridging extent (see Table II for meaning of codes 0-9). Lower three graphs are atmospheric pressure, wind speed/direction and air temperature. The data and approximate ship location arc shown in center of figure.

10

though they do not represent a time series measured at a fixed point. The date and a descriptive ship's location are indicated in the center of the figure.

The upper three plots are measures of ice concentration, thickness and the extent of ridging taken from the ship's ice observer's logs. The observation codes (0 to 9) are plotted with the higher numbers refering to higher concentration, greater thickness and more extensive ridging. The numerical description for the corresponding ice condition code is provided in Table II. The ice observations are discussed below along four track segments (Figure 1).

Table II. Ice Condition Codes for Figure 3

CONCENTRATION & EXTENT OF RIDGING			
0: <1/10, <½ Okta	5: 6/10	5 Oktas	
1: 1/10 1 Okta	6: 7-8/10	6 Oktas	
2: 2-3/10 2 Oktas	7: 9/10	7 Oktas	
3: 4/10 3 Oktas	8: 10/10	8 Oktas (with openings)	
4: 5/10 4 Oktas	9: 10/10	8 Oktas (without openings)	

THICKNESS		
0: <5 cm	5: 40-60 cm	
1: 5-10 cm	6: 60-90 cm	
2: 10-20 cm	7: 90-150 cm	
3: 20-30 cm	8: 1.5-2.5 cm	
4: 30-40 cm	9: >2.5 m	

- **1 March - 13 March 1980; North transit from ice edge to Nome**

  During this portion of the cruise ice concentration was quite
  variable, ranging from 2/10 to 10/10. An area of low concen-
  tration was encountered west of Nunivak Island early on
  4 March. Concentration tended to be consistently high (10/10)
  east of St. Lawrence Island (7-10 March) and decreased some-
  what on approaching Norton Sound on 11-12 March. Ice thick-
  ness increased from about one-half meter near the ice edge
  to about a meter or more east of St. Lawrence Island. Ridging
  extent was somewhat higher east of St. Lawrence and near Nome, than
  to the south near the ice margin.

- **15 - 20 March; Westward transit north of St. Lawrence Island**

  North of St. Lawrence Island the ice was of generally high
  concentration (10/10) often with no openings and had a thick-
  ness of 1 to 1.5m. Ridging extent was significantly greater
  here than during any other portion of the track. The break
  in the observation record (17-19 March) is a period of essen-
  tially no ship progress.

- **20 - 25 March; west and south of St. Lawrence Island**

  Ice conditions were significantly less severe west and south
  of St. Lawrence Island. Concentration was variable (2/10 to
  9/10) and the average thickness dropped to about less than
  one-half meter.

- **29 March - 3 April; transit south to the ice edge**

  As should be expected ice concentration and thickness decreased
  during the transit south from St. Lawrence to the ice edge. An
  exception was an increase in concentration, thickness and ridging
  extent in the vicinity of St. Matthews Island (30 March).

The lower three plots of Figure 3 show the atmospheric pressure, wind
speed/direction and air temperature during the cruise. During the early part
of the cruise, through 8 March, air temperatures were within $+2^{\circ}$ of $0^{\circ}C$, which
is unusually high for this area and time, with the winds from the east and often south
of east. On 9 March temperatures dropped and remained in the $-15^{\circ}C$ to $-25^{\circ}C$
range until 19 March. Winds during this period were from the northern quad-
rant and were usually less than 25 knots. During the remainder of the cruise,
temperatures hovered at about $-5^{\circ}C$ except for a short cooling period on 28 March.
Northerly winds of about 25 knots persisted from 25 March through the end of the
observation period.

12

4.3 PRELIMINARY OCEANOGRAPHIC RESULTS

4.3.1 Introduction

This section provides a few of the preliminary results from the physical oceanographic data. In general the data used is from the shipboard plots of salinity and temperature and has not been corrected or adjusted based on the salinometer or reversing thermometer measurements. Although the data is in a rather raw form, stated values are believed to be accurate to within $\pm 0.02^{\circ}C$ and $\pm 0.02^{\circ}/oo$ for temperature and salinity respectively. The analysis and discussion contained herein are not complete, but should provide ideas for future more indepth study.

4.3.2 Properly Distributions

The vertical hydrographic structure of stations within the ice fell into two general categories; vertically homogeneous and two-layer. About 40% of the stations displayed essentially homogeneous conditions in the vertical with temperature and salinity differences of less than $0.02^{\circ}C$ and $0.02^{\circ}/oo$ respectively between near surface and near bottom values. Resultant vertical stratification would be less than $0.02 \, \sigma_T$ units. These vertically homogeneous conditions occurred over a range of water depths from 15 to 75 m. The remaining stations generally can be typified as two-layer with essentially homogeneous surface and bottom layers separated by a halocline of a few meters in vertical extent. Salinity differences between the two layers were usually $0.05^{\circ}/oo$ to $0.35^{\circ}/oo$ although occasional differences of about $1.90^{\circ}/oo$ occurred within the ice and vertical changes of $> 1.00^{\circ}/oo$ were typical near the ice edge.

Salinities ranged from less than $31.0^{\circ}/oo$ in Norton Sound and along the Alaska coast near the mouth of the Yukon River to in excess of $34.0^{\circ}/oo$ at one station north of St. Lawrence Island. Temperatures at stations within the ice showed less variability than salinity, being rather uniformly cold and near the freezing point. Exceptions included warm positive temperatures outside the ice edge and warm near bottom temperatures which extended in under the ice to about the 100 m depth contour.

13

The horizontal distribution of surface and bottom layer salinities (Figures 4 and 5) appear quite similar in many respects. The highest surface and bottom salinities ($>33^O/_{OO}$) are found in the area surrounding St. Lawrence Island and at one station north of Nunivak Island. Low salinity water ($<31^O/_{OO}$) was observed at the surface and bottom in Norton Sound and near the surface along the Alaska coast near the Yukon River delta. A boundary of high horizontal salinity gradients separating these high and low salinity waters extends southward across the mouth of Norton Sound towards Nunivak Island. Surface salinities in the middle and outer shelf regions (southwest of the 50 m cont....) were more uniform at about $32^O/_{OO}$; slightly less than $32^O/_{OO}$ over the southeastern shelf and somewhat greater than $32^O/_{OO}$ over the more northwesterly portion of the shelf. Stations across the northwestern shelf show high salinity (and warm, $>0^OC$) bottom water extending under the ice to the 100 m depth contour.

A simple measure of the vertical stratification was constructed by computing the difference in sigma-T between the surface and bottom layers. At these low temperature and for the range of temperatures and salinities encountered, sigma-T is essentially a function of only salinity and not temperature ($\Delta\sigma_T/^OC \cong 0.05$; $\Delta\sigma_T/^O/_{OO} \cong 0.80$). The horizontal distribution of $\Delta\sigma_T$ is shown in Figure 6. Two-layer stations with $\Delta\sigma_T>0.02$ are contoured, while the remaining are essentially vertically homogeneous. Stations seaward (southwest) of about the 50 m contour (middle and outer shelf regions) were two-layered with stratification increasing toward the ice edge. Stations in Norton Sound and in a region extending towards the eastern end of St. Lawrence were somewhat stratified as were those along the coast south of the Yukon River. Isolated stations with significant stratification occurred both north and south of St. Lawrence.

4.3.3 Temperature - Salinity Correlations

The correlation between temperature and salinity values for the surface and bottom waters is shown in Figures 7 and 8. The surface layer T-S plot includes points from all stations within the ice (Stations 10-79 inclusive). The bottom layer T-S plot excludes stations near the ice edge which

14
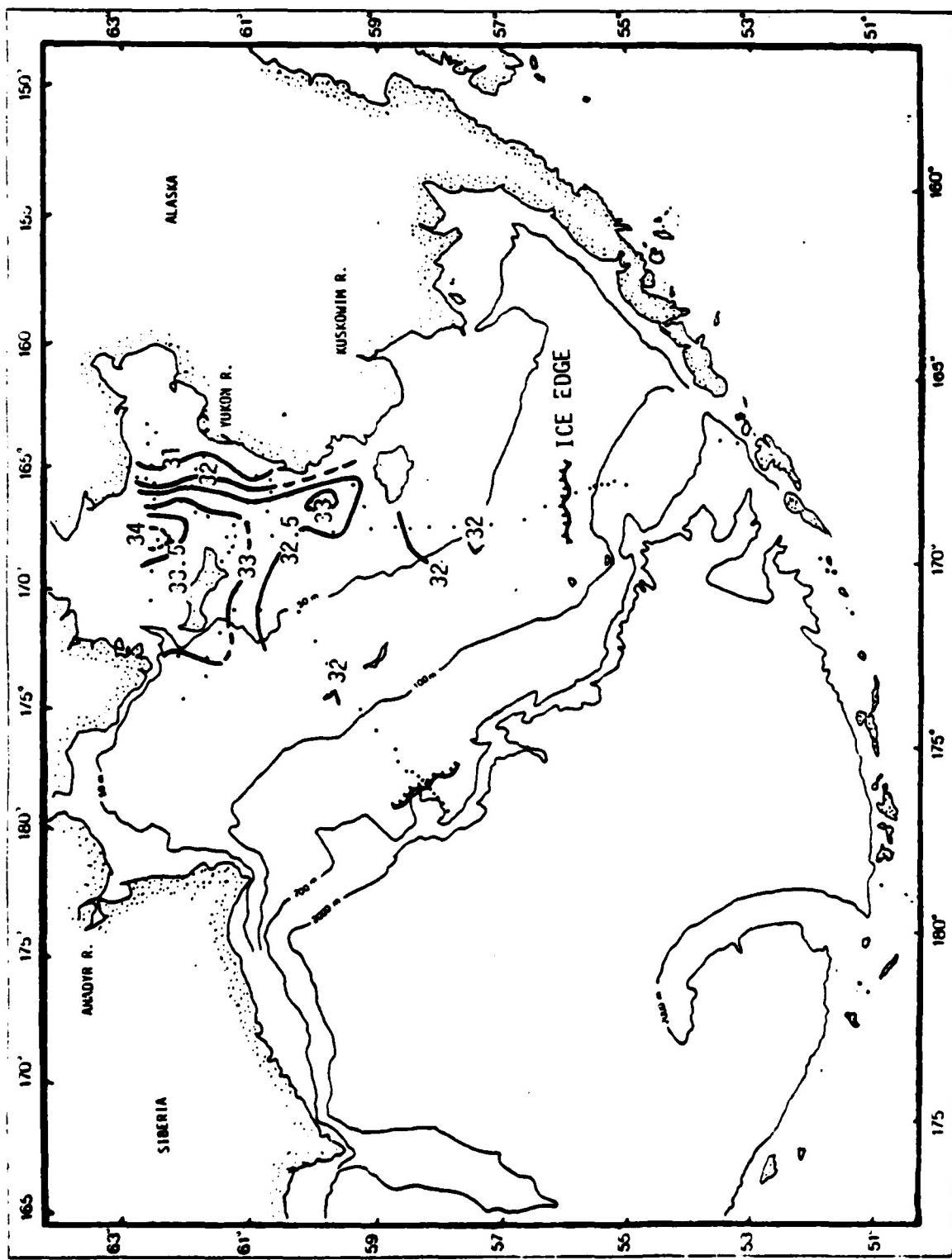
Figure 4. Horizontal distribution of surface layer salinity. Note contour interval is 0.5°/oo for salinities greater than 32°/oo; 1°/oo for salinities less than 32°/oo.
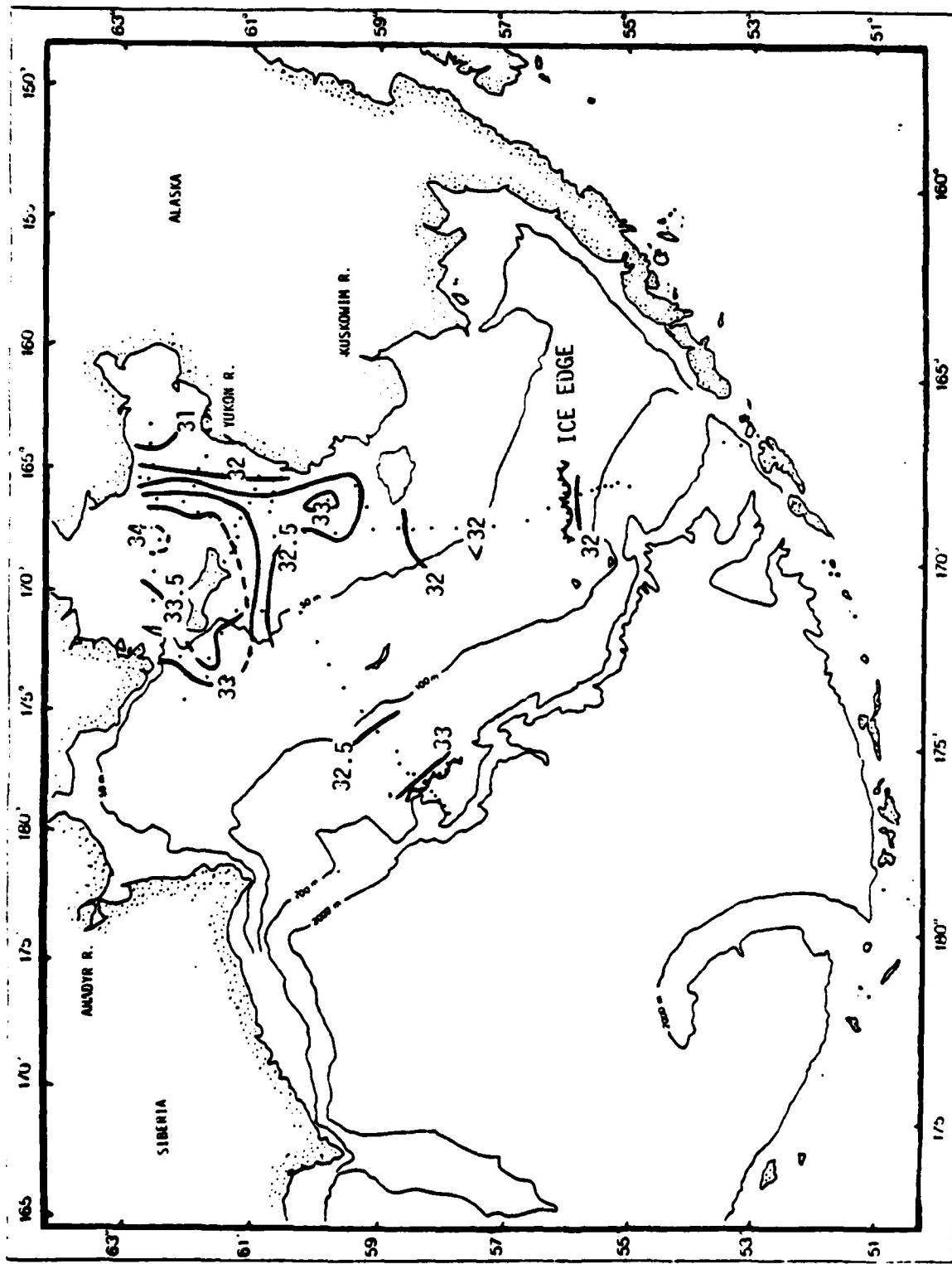
Figure 5. Horizontal distribution of bottom layer salinity. Note contour interval is 0.5°/oo for salinities greater than 32°/oo; 1°/oo for salinities less than 32°/oo.

16
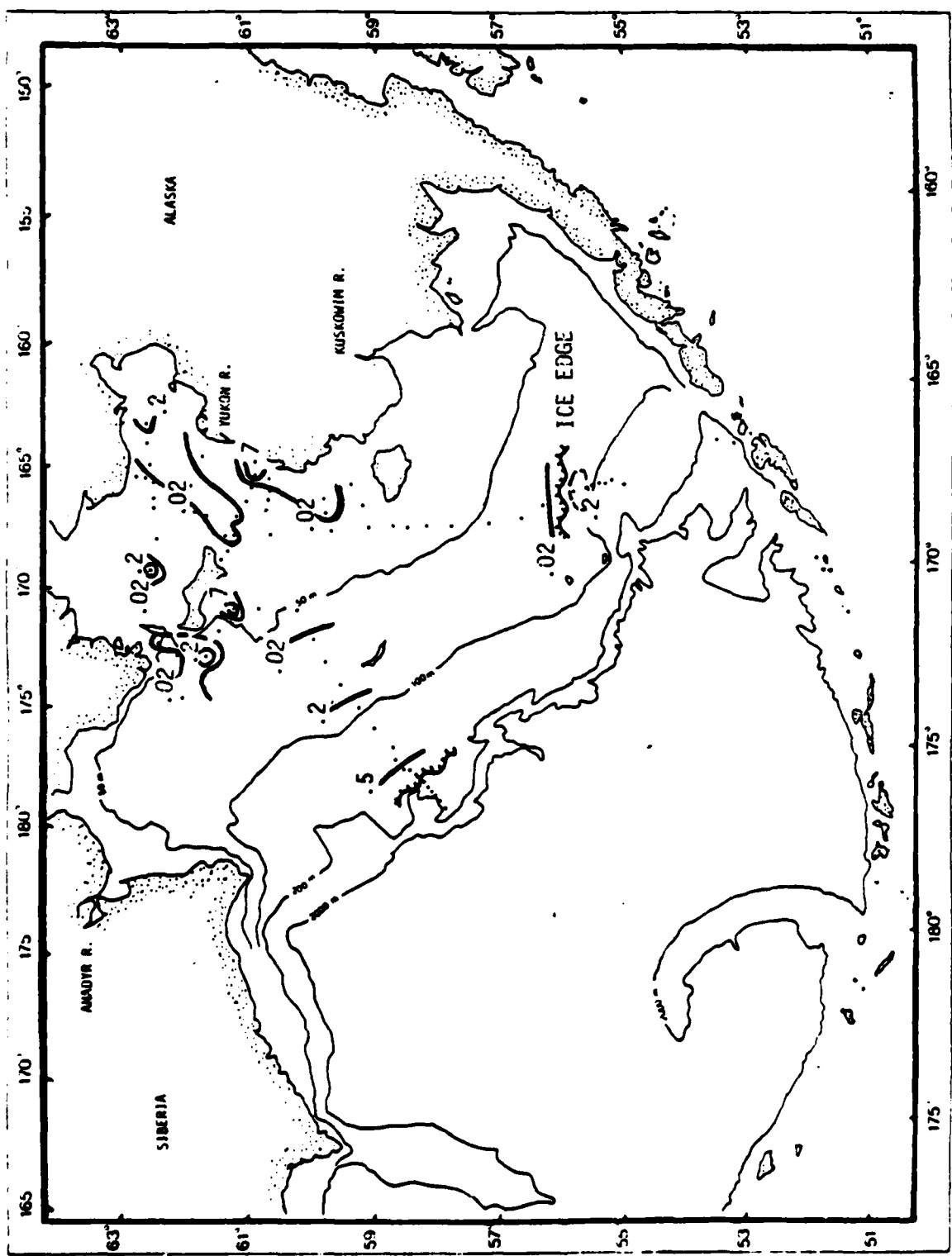
Figure 6. Horizontal distribution of the sigma-t difference, $\Delta\sigma_t$, between the surface and bottom layers contoured at 0.02, 0.20 and 0.50 σ_t unit intervals. Uncontoured stations were essentially vertically homogeneous ($\Delta\sigma_t < 0.02$).

17
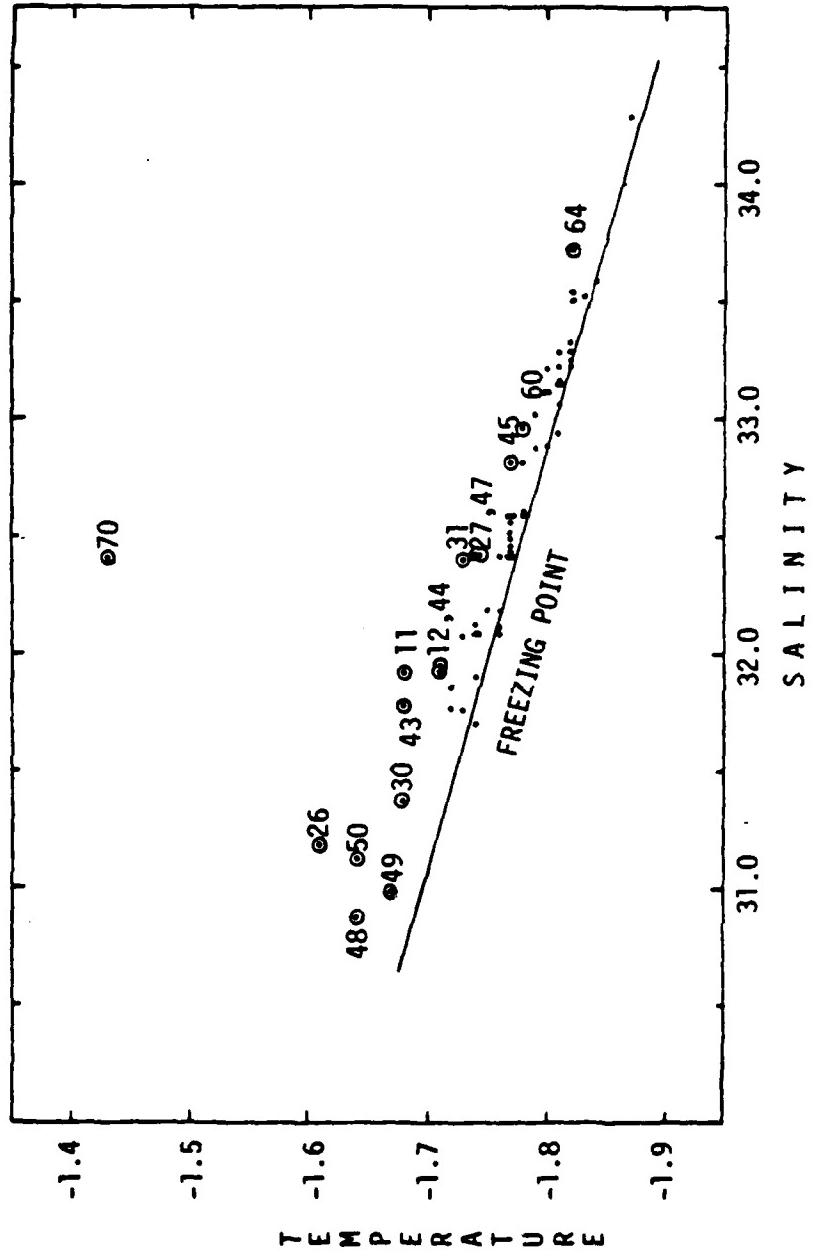
Figure 7. Temperature - Salinity correlations for surface layers at stations within ice pack (Stations 10-79). The freezing point line is from Doherty and Kester (1974).

18
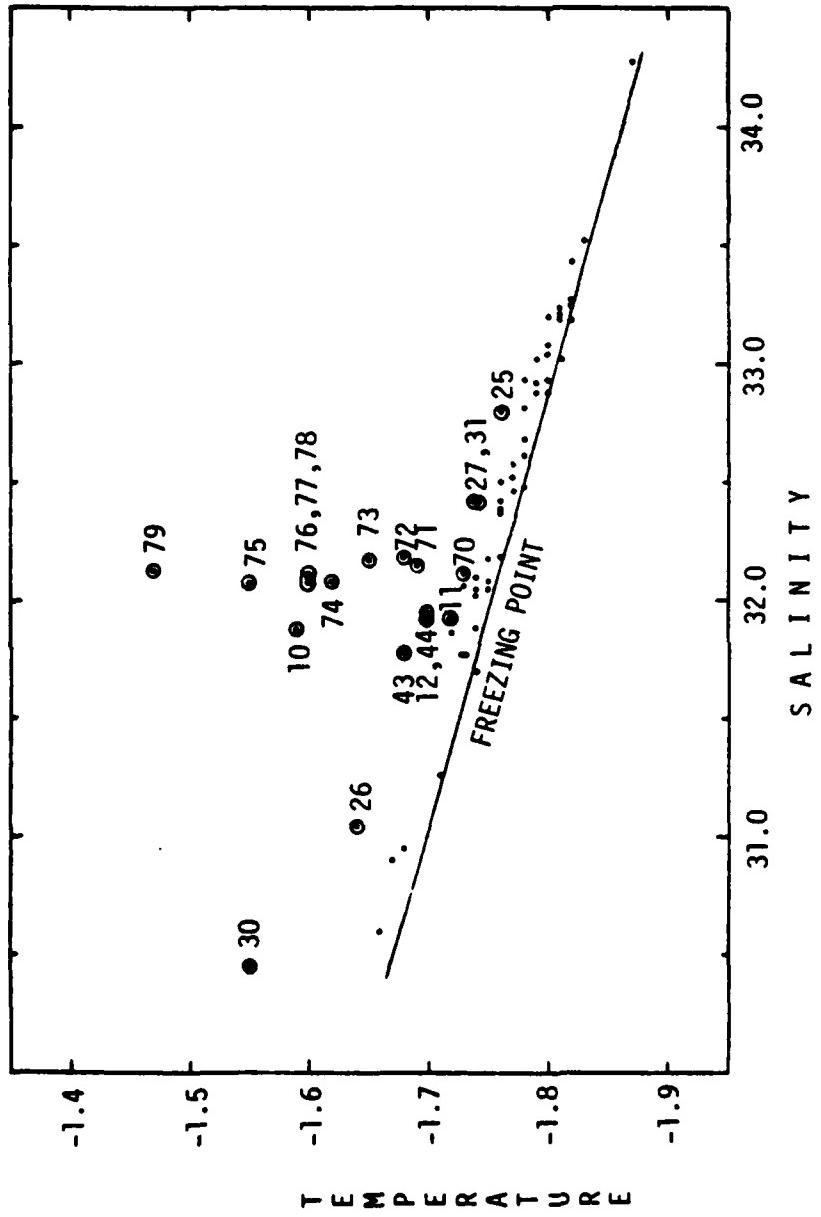
Figure 8. Temperature - Salinity correlations for bottom layers at stations in the ice pack less Stations 10 and 71-79, which had temperatures >-1.4°C. The freezing point line is from Doherty and Kester (1974).

had significantly elevated temperatures of >-1.4°C (i.e., Stations 10 and 71-79). Each plot includes the freezing point curve from Doherty and Kester (1974).

Surface layer temperatures within the ice ranged from -1.47°C (Station 70) to a minimum at Station 55 of -1.87°C. At the majority of the stations, surface layer temperatures were within 0.02°C of the freezing point line (Figure 7). Stations with temperature in excess of 0.02°C above the freezing point are identified on Figure 7 and their geographic distribution is indicated in Figure 9. Surface layers with temperatures significantly above the freezing point appear to be concentrated in two areas; along the Alaska coast south of Norton Sound and near the ice edge.

Seven stations along the Alaska coast south of the Yukon delta had surface layer temperatures above freezing. Of these seven stations, six were associated with the low salinity (<32.5°/$_{oo}$) water along the coast (Figure 4). The near shore, lowest salinity surface layers tended to be somewhat more elevated above their respective freezing points than were surface layers at adjacent stations located farther from shore with higher salinities. This can be seen in Figure 7 by observing the T-S trends from stations 30 to 31, 43 to 44 and 26 to 27 to 25 which in each case illustrate the T-S changes proceding outward from the coast.

The second region with surface layer temperatures above the freezing point was located near the ice edge. For the eastern crossing of the ice edge (essentially at station 10) surface layer temperatures were elevated above freezing for a distance of about 80 km into the ice pack (Stations 11 and 12). For the western crossing (near Station 79) surface layer temperatures were elevated above freezing for nearly 200 km into the ice pack (Stations 70 through 79). The trend in T-S characteristics proceeding from the ice edge (Stations 10 and 79) into the pack ice (toward Stations 12 and 70) was one of decreasing temperature (although not always monotonic) with perhaps a slight increase in salinity.

Because of the warm, high salinity water which extended under the ice pack during the western crossing, bottom layer temperatures covered a significantly greater range than did the surface layers, -1.87°C to >3.0°C.
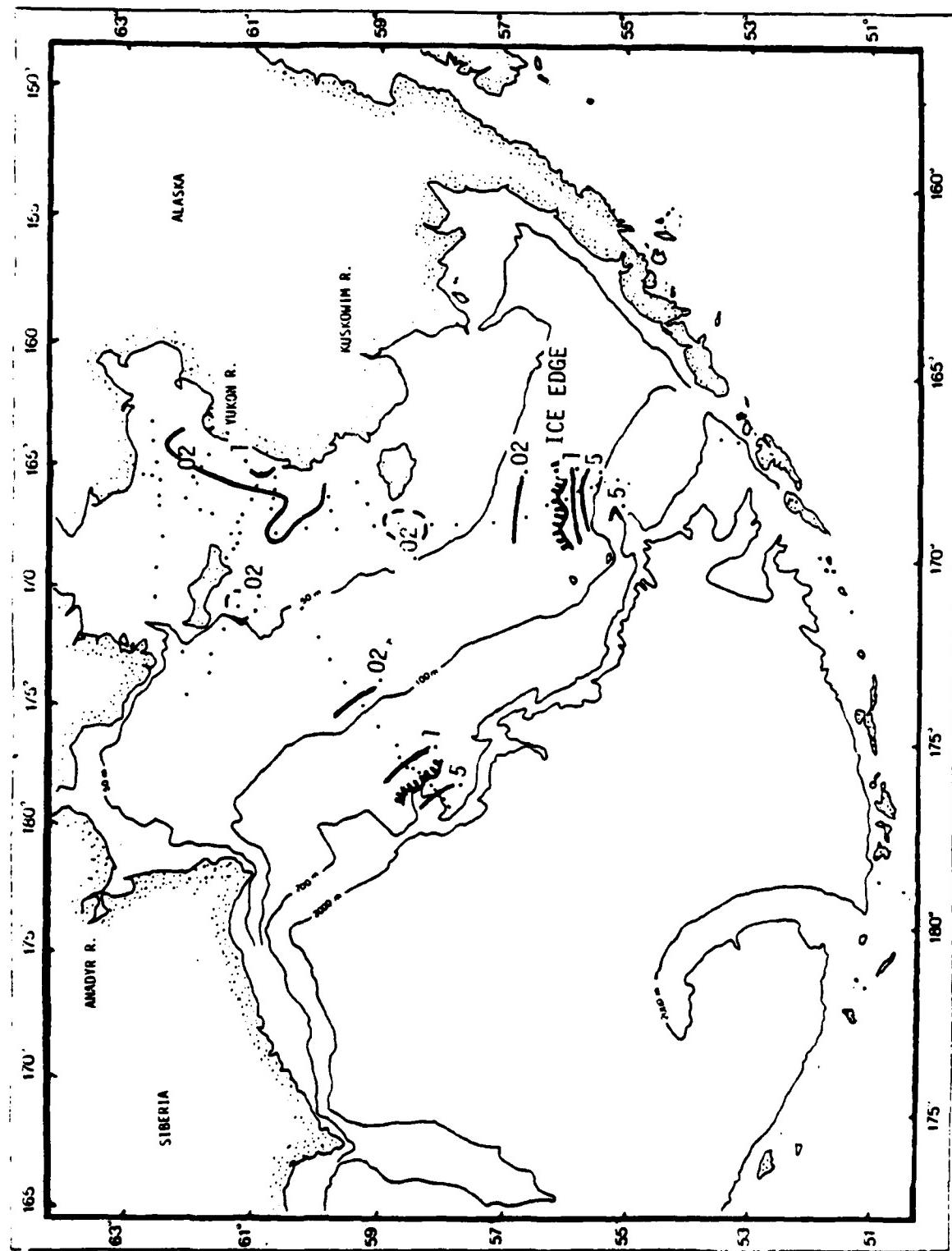
Figure 9. Geographic distribution of surface layer temperatures which were 0.02°C above freezing point (temperature observed - freezing point for observed salinity). Freezing point calculated from Doherty and Kester (1974).

Stations with bottom layer temperatures of $>0.02^{o}C$ above the freezing point have been identified on Figure 8 and their geographic distribution is indicated in Figure 10. Near the ice edge the spatial extent of bottom layers with temperatures above freezing is similar to that of the surface layers although the magnitude of departure is greater in the lower layers because of the warm water extending in order the ice to the 100 m contour. The region near the Yukon delta with above freezing bottom layer temperatures is extended to the north and covers those stations in Norton Sound. As was the case for the surface waters, there appears to be general tendency for the greatest temperature departures from freezing to be associated with the lower salinities.

It seems reasonable to explore the T-S relationship observed within the ice pack under freezing conditions in more depth. A strong motivation is the comparison of the field data with various formula for computing the freezing point. Which set of stations to use in such an analysis presents a major problem. Almost any criteria (such as using points within $\pm 0.02^{o}C$ of a calculated freezing point) is bound to bias the results. As a preliminary attempt stations which seemed above the freezing point for a good physical reason (i.e., near the ice edge, near the Yukon delta and the bottom layers of Norton Sound) were eliminated. A linear regression was computed based on the remaining points (i.e. those not contoured in Figures 9 and 10) and the results are tabulated in Table III.

As expected, and as is obvious from Figures 7 and 8 the slope of the T-S correlations (0.0580 and 0.0582 for upper and lower layers) is very close to that of the Doherty and Kester (1974) formula which in the range $30-35^{o}/_{oo}$ is 0.0563 to 0.0570. Figure 11 is a comparison of some different freezing point measurements and calculations with the regressions from this field data. Appendix B describes the freezing point formulas and data in more detail. The values plotted are differences between the Doherty and Kester (1974) formula and the data regressions and other formulas. For the range of salinities considered here ($30-35^{o}/_{oo}$) the Doherty and Kester formula predicts the lowest freezing point. The regressions on the data
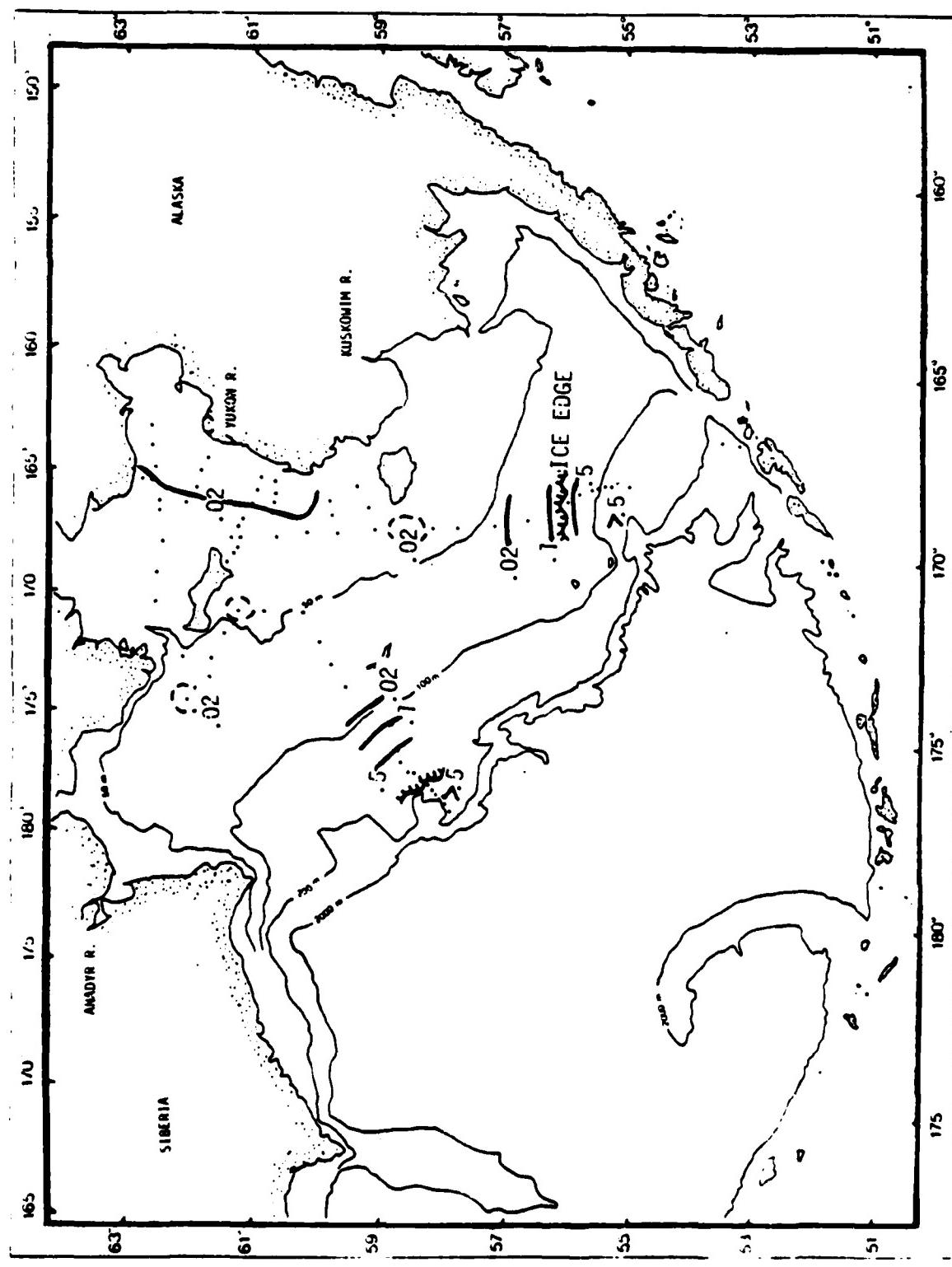
Figure 10. Geographic distribution of bottom layer temperatures which were >0.02°C above the freezing point (temperature observed – freezing point for observed salinity). Freezing point calculated from Doherty and Kester (1974).

23
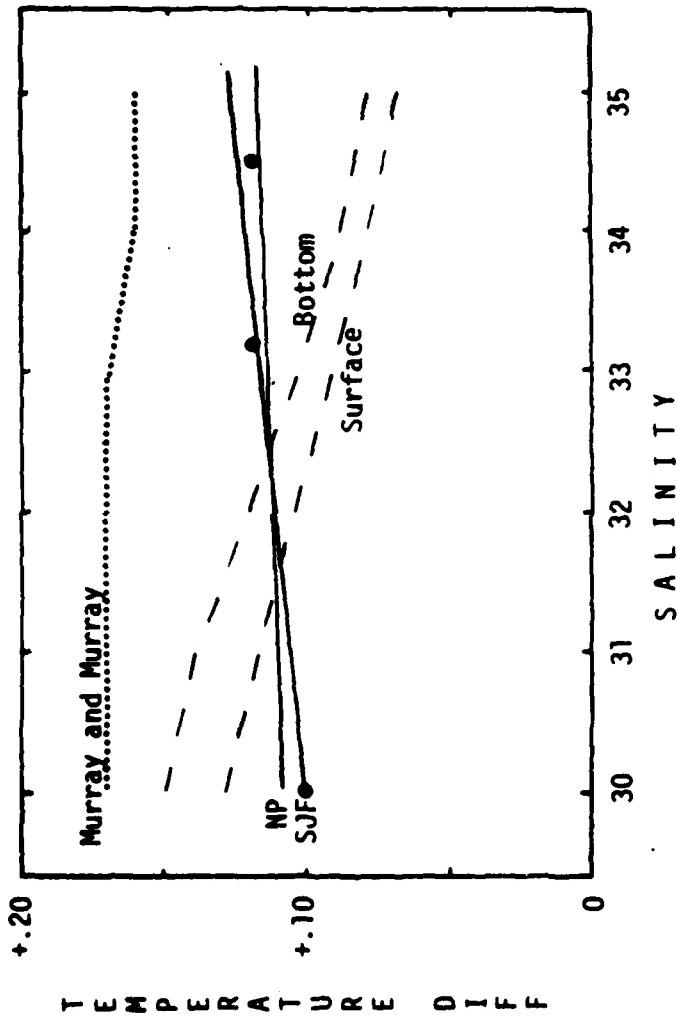
Figure 11.   Comparison of data regressions for surface and bottom
layer temperature-salinities of stations with pre-
sumably near freezing conditions to various freezing
point calculations. The regressions and freezing point
calculations are expressed as differences from the
Doherty and Kester (1974) formula over the salinity
range 30 to 35%.

Table III. Results of T-S Regression for Selected Stations

	UPPER LAYER	LOWER LAYER
MEAN SALINITY	32.52	32.69
STD. DEV. (SAL)	0.72	0.65
MEAN TEMPERATURE	-1.77	-1.78
STD. DEV. (TEMP.)	0.04	0.04
SLOPE	-0.0580	-0.0582
INTERCEPT	0.115	0.123
CORRELATION COEFFICIENT	-.94	-.98

lie about $0.014^{\circ}C$ above the D-K freezing point at low salinities and $0.008^{\circ}C$ above at higher salinities. The regressions are within $\pm 0.006^{\circ}C$ of the Hansen data (as well as the SJF and NP formulas); being higher at low salinities and below at the higher salinities. The trend in the data for temperatures to be higher relative to the computed freezing points at the lower salinities may be a result of the general oceanographic conditions encountered during the cruise (i.e., the higher temperatures were usually associated with the lower salinities south of St. Lawrence and near the Yukon delta).

4.3.4   Vertical Sections Across the Ice Edge

Vertical cross sections of temperature and salinity were constructed from data at the two lines of stations which crossed the ice margin. Stations 3 through 12 were occupied over a 32-hour period during the transit inbound to the ice (1230Z 29 FEB - 2040Z 1 MAR 80). The section for Stations 3 through 12 (Figure 12) is approximately 200 km long with a station spacing of about
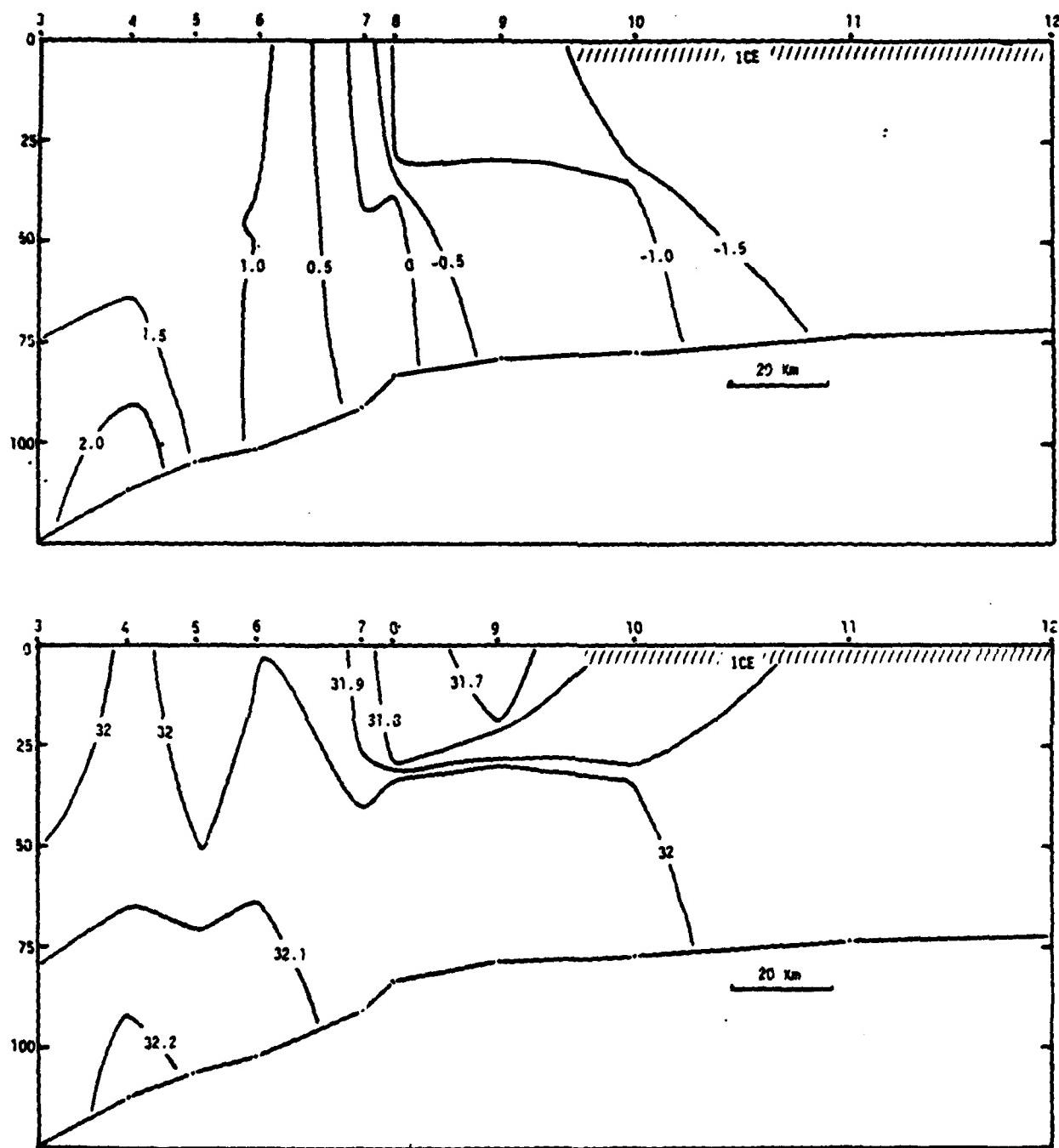
Figure 12. Vertical sections of temperature and salinity across the ice edge
(Stations 3 through 12). Temperature contoured at 0.5°C intervals,
salinity at 0.1 intervals.

40 km within the ice pack and about 20 km or less outside the ice. The second section (Stations 69 through 83) was occupied on the outbound transit during the period 2000Z 30 MAR to 1530Z 2 APR 80. The bulk of the stations near the ice margin (74-83) were occupied in a 24-hour period. The section for Stations 69 through 83 (Figure 13) is 300 km in length with a station spacing of 50 km in the ice and about 10 km in the vicinity of the ice edge.

The first ice margin crossing (Stations 3-9) occurred over the Southeastern Bering Sea Shelf between the 100 and 50 m contours. The ice edge was encountered between Stations 9 and 10 over water of about 80 m depth (Figure 12). The -1.5°C isotherm was nearly coincident with the ice edge at surface and sloped in under the ice intersecting the bottom about 40 km under the ice pack. The transition from the cold ($<-1.5^{\circ}$C) water under the ice to the warm ($>1.0^{\circ}$C) ice free waters to the south took place over a distance of 60 km. In the southern portion of the transition (Stations 6 and 7) the isotherms were nearly vertical and vertical stratification was rather low ($\Delta\sigma_t \sim .1$). Near the ice edge (Stations 8-10) a lens of relatively fresh water ($<31.8^{\circ}/_{00}$) can be discerned at the surface.

The second ice crossing took place approximately 240 n.m. northwest of the first across the central Bering Sea Shelf. The ice edge was encountered at Station 79 in a water depth of about 150 m. The hydrographic structure of the second ice margin crossing (Figure 13) displayed some similarities to the first section (Figure 12) however there were significant differences. The -1.5°C isotherm intersected the surface near the ice edge but extended nearly 200 km under the ice prior to reaching the bottom. Positive near bottom temperatures were found 150 km in under the ice pack. The surface layer, above the -1.5° isotherm, was nearly homogeneous in both temperature and salinity. Rather than a transition from cold to warm water of vertically oriented isotherms ($-.5^{\circ}$C to $+1.0^{\circ}$C) as in the first section, the isotherms sloped in under the ice pack for nominally 160 km. The result is a nearly homogeneous low salinity, cold surface layer separated from a warm more saline bottom layer by a sharp halocline/thermocline of a few meters in vertical extent. As was the case of the first crossing, a near surface low salinity lens ($<32.12^{\circ}/_{00}$ in this case) is located near the ice edge.

27
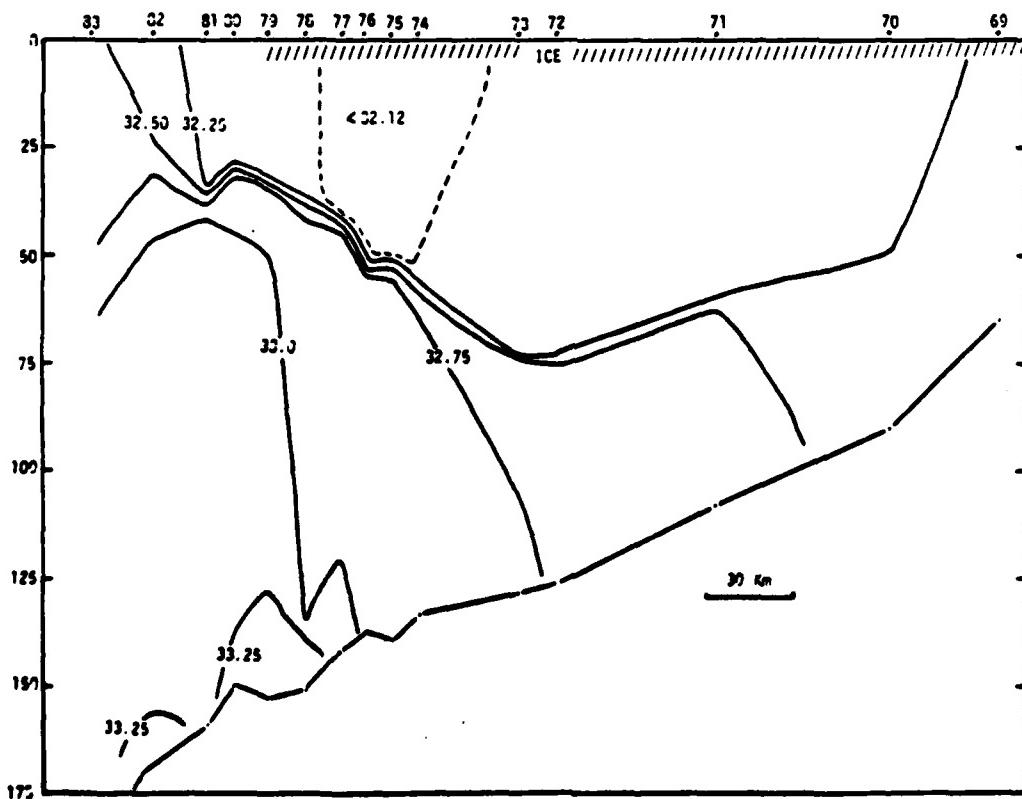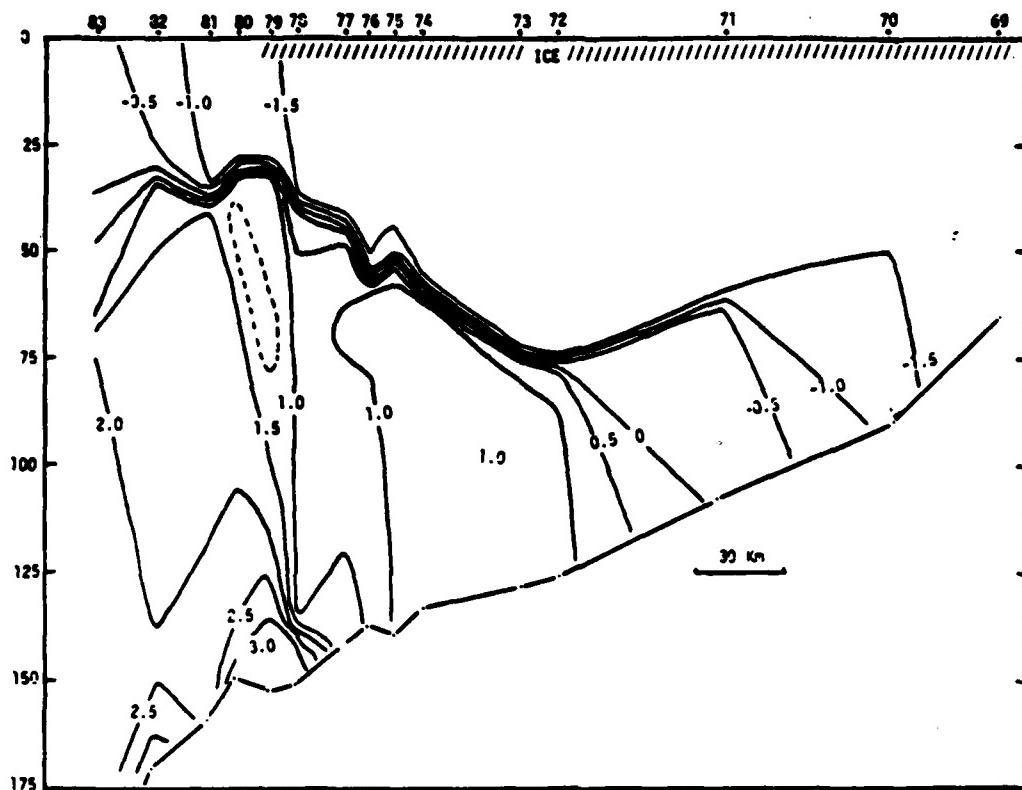
Figure 13. Vertical sections of temperature and salinity across the ice edge (Stations 69 through 83). Temperature contoured at 0.5°C intervals, salinity at 0.25 intervals.

The basic similiarity between the two sections is the freshening of the surface waters near the ice margin while significant differences include the water depth at the ice edge and the attendant hydrographic structure of the transition from cold to warm water which was one of vertically oriented isotherms in one case and a sloping halocline/thermocline in the other.

The transition of surface layer properties from open water (outer shelf) conditions to underice freezing conditions is further illustrated in Figure 14 which is a plot of surface layer temperature and salinity for stations making up the section of Figures 12 and 13. The arrows indicate the progression from open water to under ice stations. In both cases, proceeding from open water to underice stations the T-S correlation moves to a salinity minimum which is somewhat elevated above freezing (Station 9 and Stations 74-76) and then salinity increases and temperature decreases to the freezing point line (Stations 11-12 and 69) representative of underice conditions.

Lateral mixing of open water and underice water masses would fall along a straight line between Stations 3-6 and 11-12 for the first section and Station 83 (or perhaps a warmer, saltier water mass) and Station 69 in the second section. Salinity enhancing processes such as freezing or upwelling near the ice edge would presumably cause a bowing of the T-S correlation to the right of the straight mixing line. The left bending of the T-S correlation (toward low salinities) observed in both T-S correlations suggests a third component in the mixing relationship which is cold and relatively fresh.

A potential source for the cold fresh water is meltwater generated locally as the ice contacts the relatively warm open water.

4.3.5   Discussion

The process of wintertime ice formation on the Bering Sea shelf results in a nearly homogeneous water column with a temperature very near the freezing point. Continued ice formation in a particular area during the winter can result in salinities which are significantly greater than summertime values. A brief, qualitative comparison of the horizontal salinity distributions in Figures 3 and 4 to typical mid-summer bottom layer salinities
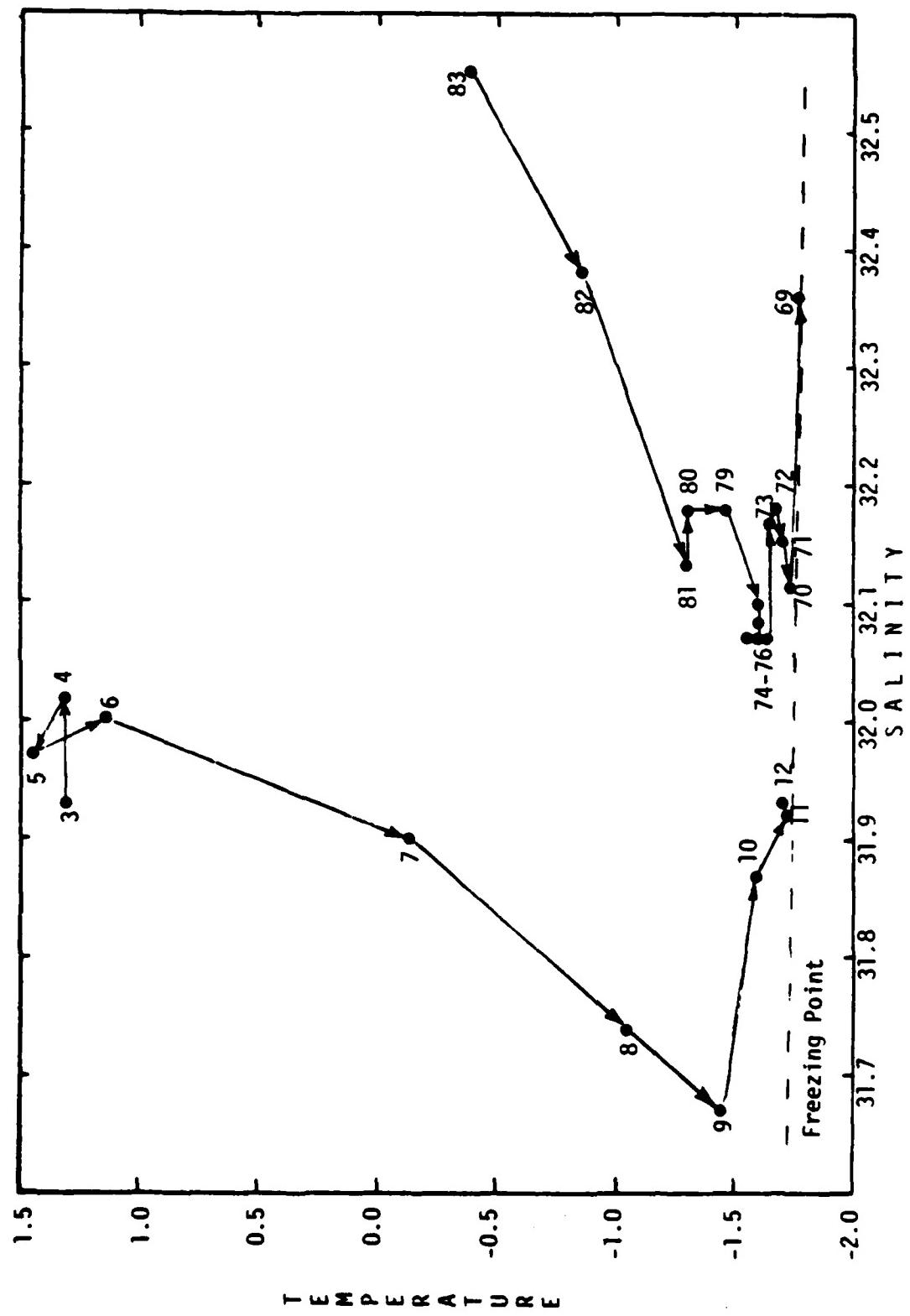
Figure 14. T-S characteristics of the surface layers at stations taken across the ice margin. The arrows indicate the progression from open water across the ice margin to the underice stations.

(Ohtani (1969), Coachman, Aagaard, and Tripp (1975)) suggest that the ice formation processes have significantly enhanced the wintertime salinities in the region surrounding St. Lawrence Island and to some extent southeast of St. Lawrence Island toward Nunivak Island. Based on the observations of this cruise, the wintertime salinities appear to be about .5 to 1.5$^o/_{oo}$ greater than typical summertime values. Neglecting the affects of other processes which could modify the salinity such as advection, this is roughly equivalent to the production of 1-2 m of ice in water depths of 30-50 m during the winter. This potentially ice productive region generally corresponds to the areas (Figures 9 and 10) with temperatures consistently near the freezing point.

In contrast, the salinities observed during this cruise over the middle and outer shelf regions (between the 50 m contour and the shelf break) did not seem obviously different from typical values during other seasons. Further, surface layer temperatures seaward of the 50 m depth contour were usually above freezing. Thus, based on the observed temperature and salinity distributions, and neglecting other possible modifying processes, the middle and outer shelf regions do not appear as obvious ice producing areas.

The hydrographic structure associated with the two ice edge crossings were noticeably different, particularly with respect to the transition from the cold under ice water mass to the southern warmer waters. For the first crossing (Figure 12), in relatively shallow water over the southeastern shelf, the transition consisted of nearly vertically oriented isotherms. The second crossing occurred in deeper water over the central area of the shelf. In this case the transition between warm saline and cold fresh water consisted of a sharp halocline/thermocline which sloped in under the ice for nearly 160 km. The temperature-salinity characteristics of the surface layers (Figure 14) associated with both crossings suggest a fresh-water component in the mixing relationship near the ice edge. A possible explanation, which is consistent with this T-S relationship and the observation that surface layer temperatures are significantly above freezing for several 10s of km or more into the ice pack, is that the southern ice margin is in general melting and not a region of ice production.

REFERENCES

1. Coachman, L. K., K. Aagaard, and R. B. Tripp, 1975. Bering Strait; The Regional Physical Oceanography. University of Washington Press, Seattle., 172 pp.

2. Doherty, B. T. and D. R. Kester, 1974. Freezing Point of Seawater. J. Mar. Res. 32(2):285-300.

3. Neumann, G. and W. J. Pierson, Jr., 1966. Principles of Physical Oceanography. Prentice-Hall, Inc., Englewood Cliffs, NJ, 545 pp.

4. Ohtani, K., 1969. On the Oceanographic Structure and the Ice Formation on the Continental Shelf in Eastern Bering Sea. Bull, Fac. Fish., Hokkaido University, 20(2):94-117 (in Japanese).

5. Sverdrup, H. U., M. W. Johnson, and R. H. Fleming, 1942. The Oceans; Their Physics, Chemistry, and General Biology. Prentice-Hall, Inc. Englewood Cliffs, NJ, 1087 pp.

APPENDIX A - STATION DATA

This appendix tabulates data pertinent to the oceanographic stations including position, date-time (GMT) and the sounding in meters. The platform column indicates whether the cast was taken from the ship, helicopter or the ice. In the last three columns, X's denote the instrument system(s) used and those stations where a nansen bottle was utilized.

APPENDIX A - STATION DATA

STATION	POSITION		DATE	TIME(Z)	DEPTH(m)	PLATFORM	NBIS CTD	LP	NANSEN
1	54-20.0N	166-17.0W	29 FEB 80	0019	778	Ship	X		
2	54-36.0	166-12.0		0236	403		X		X
3	56-15.0	167-16.0		1230	128		X		X
4	56-23.5	167.08.0		1502	112		X		
5	56-30.0	167-12.0		1636	126		X		X
6	56-37.0	167-14.0		1720	102		X		X
7	56-47.5	167.20.0	29 FEB 80	1849	91		X		X
8	56-50.0	167-23.0	1 MAR 80	0054	82		X		X
9	57-01.0	167-30.4		0239	79		X		X
10	57-14.5	167-39.7		0625	77		X	X	
11	57-35.7	167-55.0		1143	73		X		X
12	57-57.0	168-10.0	1 MAR 80	2038	72		X		X
13	58-30.0	168-16.0	3 MAR 80	0400	59		X	X	
14	59-05.0	168-08.0	3 MAR 80	1830	42		X		
15	59-36.0	168-10.0	3 MAR 80	2348	40		X		X
16	59-52.1	168-16.5	4 MAR 80	0406	37		X		
17	60-03.3	168-12.8		0522	33		X		
18	60-34.0	169-09.0		0901	31		X		
19	60-41.5	167-28.0		1600	24		X		
20	60-49.0	166-48.0		1926	23		X		
21	60-18.0	167-07.0	4 MAR 80	2311	24		X		
22	61-16.0	167-36.0	5 MAR 80	0115	26		X		
23	61-10.0	168-08.0		0330	30		X		
24	61-43.0	168-04.0		0852	33		X		
25	62-09.7	168-09.0		1538	20	Ship	X		
26	62-09.0	166-16.0		1944	10	Helo		X	
27	62-12.0	166-39.0		2002	15			X	
28	62-14.5	166-59.5		2014	31			X	
29	62-19.2	169-22.0	5 MAR 80	2025	25			X	
30	62-26.0	166-02.0	6 MAR 80	0150	12			X	
31	62-30.0	166-36.0	6 MAR 80	0200	12	Helo		X	

A-2

STATION	POSITION		DATE	TIME(Z)	DEPTH(m)	PLATFORM	NBIS CTD	LP	NANSEN
32	62-40.0N	167-00.0W	6 MAR 80	1305	31	Ship	X		X
33	62-44.0	167.30.0	6 MAR 80	2305	29	Ice		X	
34	62-52.0	167-47.0	7 MAR 80	1852	28	Ship	X		
35	62-52.0	168-05.0	8 MAR 80	0536	34	Ship	X	X	X
36	62-52.0	168-05.0	8 MAR 80	1711	31	Ship	X		
37	62-55.7	168-24.0	9 MAR 80	0150	29	Helo		X	
38	63-03.5	169-05.0	9 MAR 80	0224	40	Helo		X	
39	62-59.0	168-44.0	9 MAR 80	0235	36	Helo		X	
40	62-55.0	168-14.0	9 MAR 80	0920	40	Ship	X	X	
41	62-16.0	167-28.0	10 MAR 80	0712	33	Ship	X		
42	63-27.0	167-11.0	10 MAR 80	2139	27	Ship	X		
43	63-17.0	165-23.9	11 MAR 80	0125	17	Helo		X	
44	63-24.7	165-40.3		0139	22	Helo		X	
45	63-32.5	166-15.0		0157	25	Helo		X	
46	63-43.0	166-56.0		0218	28	Helo		X	
47	64-05.0	166-00.0		1813	21	Ship	X		X
48	64-07.0	163-47.0		2048	16	Helo		X	
49	64-06.7	164-36.7		2108	14	Helo		X	
50	64-07.0	165-18.0		2126	17	Helo		X	
51	64-14.5	165-55.0	11 MAR 80	2220	22	Ship	X		X
52	64-24.0	165-50.0	12 MAR 80	0745	26		X		
53	64-04.0	166-31.0	14 MAR 80	1110	31		X		
54	64-06.5	166-59.0	14 MAR 80	1342	31		X		
55	64-05.0	168-07.0	15 MAR 80	1850	38		X		
56	64-16.0	169-17.0	19 MAR 80	0659	42		X		X
57	64-17.0	170-30.0	19 MAR 80	1432	31		X		
58	64-03.0	172-06.0	20 MAR 80	1720	49		X		X
59	63-49.0	172-46.0	20 MAR 80	2010	35		X		
60	63-45.0	174-15.0	20 MAR 80	2340	42		X		
61	63-22.0	173-24.0	21 MAR 80	0230	65		X		
62	63-19.0	172-40.0	21 MAR 80	0713	60	Ship	X		

STATION	POSITION		DATE	TIME(Z)	DEPTH(m)	PLATFORM	NBIS CTD	LP	NANSEN
63	63-08.0N	171-54.0W	21 MAR 80	1007	58	Ship	X		
64	62-52.0	171-00.0	21 MAR 80	1330	47		X		
65	62-25.0	171-00.0	21 MAR 80	1742	41		X		X
66-1	61-49.0	171-01.0	24 MAR 80	1545	51		X		X
66-2	61-52.0	171-01.0	25 MAR 80	0754	51		X		
66-3	61-52.0	171-01.0	25 MAR 80	0812	51		X		
66-4	61-52-0	171-01.0	26 MAR 80	0300	52			X	
66-5	61-56.6	171-19.6	27 MAR 80	0300	52			X	
67	61-36.0	172-08.0	28 MAR 80	1915	58			X	
68	61-19.0	172-52.0	29 MAR 80	2030	64		X	X	X
69	61-01.0	173-40.0	30 MAR 80	2002	65		X	X	
70	60-42.0	174-25.0	31 MAR 80	1109	89		X	X	X
71	60-24.0	175-08.0	31 MAR 80	2111	108		X	X	X
72	60-03.5	175-57.5	1 APR 80	0514	126		X		
73	60-01.0	176-04.0	1 APR 80	0621	128		X		
74	59-54.0	176-30.0	1 APR 80	1553	133		X		
75	59-49.0	176-30.0	1 APR 80	2025	139		X		
76	59-45.0	176-35.0	2 APR 80	0028	137		X		
77	59-42.0	176-45.0		0159	139		X		
78	59-39.0	176-53.0		0412	151		X		
79	59-33.0	177-02.0		0916	152		X		
80	59-29.0	177-07.0		1031	149		X		
81	59-26.0	177-14.0		1136	159		X		
82	59-20.0	177-24.0		1327	170		X		
83	59-16.0	177-45.0	2 APR 80	1537	278	Ship	X		

APPENDIX B - FREEZING POINT FORMULAS

The freezing point formulas used in constructing Figure 11 are summarized below:

- Doherty and Kester (9174)

$$T_f(^\circ C) = -0.0137 - 0.051990S - 0.00007225S^2 - 0.000758Z$$

where S = Salinity $(^\circ/_{oo})$ and Z = depth in meters (Z=0 for these calculations.

- Neuman and Pierson (1966) (NP)

$$T_f(^\circ C) = -0.0085 - 0.064633\sigma_0 - 0.0001055\sigma_0^2$$

$$\sigma_0 = -0.093 + 0.8149S - 0.000482S^2 + 0.0000068S^3$$

Combining above and dropping terms of order S^4 and greater.

$$T_f(^\circ C) = 0.00259 - 0.05265S - 0.0000389S^2 - 0.000000356S^3$$

where S = Salinity $(^\circ/_{oo})$

- Sverdrup, Johnson and Fleming (1942) (SJF)

$$T_f(^\circ C) = -0.0966Cl - 0.0000052Cl^3$$

$$S = 0.03 + 1.805Cl$$

Combining above

$$T_f(^\circ C) = 0.0016 - 0.05352S + 7.958 \times 10^{-8} S^2 - 8.84 \times 10^{-7} S^3$$

where S = Salinity $(^\circ/_{oo})$

APPENDIX B - FREEZING POINT FORMULAS (Continued)

- Murray and Murray

    Data referred to by Doherty and Kester (1974) and presented in graphical format. Also from Table 1.5-1, Handbook of Marine Science.

- Hansen

    Data points taken from Doherty and Kester (1974).